AN ELEMENT BASED CONSERVATIVE APPROACH USING UNSTRUCTURED GRIDS IN CONJUNCTION WITH A CHEMICAL FLOODING COMPOSITIONAL RESERVOIR SIMULATOR

Leonardo Karpinski, leonardo@sinmec.ufsc.br
Clovis Raimundo Maliska, maliska@sinmec.ufsc.br
Federal University of Santa Catarina, Department of Mechanical Engineering, Florianópolis/SC, Brazil, 88040-900

Francisco Marcondes, marcondes@ufc.br
Federal University of Ceará, Department of Metallurgical and Material Sciences, Fortaleza/CE, Brazil, 60455-760

Mojdeh Delshad, delshad@mail.utexas.edu
Kamy Sepehrnoori, kamys@mail.utexas.edu
The University of Texas at Austin, Department of Petroleum and Geosystems Engineering, Austin/TX, USA, 78712

Abstract. An investigation of the Element-based Finite Volume Method (EbFVM) applied to a chemical flooding compositional reservoir simulator is presented. The method employs two-dimensional unstructured grids using triangular and/or quadrilateral elements, such that complex reservoir geometries can be easily represented. To obtain the approximate equations for the control volumes, first each element is divided into three or four portions (sub-control volumes) according to the element type. Each control volume is formed by sub-control volumes of neighboring elements using the cell vertex construction. This procedure results in a convenient way to build grids that represent reservoir heterogeneities. Although the method performs operations at element level, it preserves the essence of conventional finite volume method, that is, the construction of approximate equations that guarantee the conservation of physical quantities. Finally, a comparison of the proposed method and the finite difference method originally used in the simulator for application in solving reservoir simulation case studies is presented.

Keywords: EbFVM, chemical compositional model, unstructured grid, petroleum reservoir simulation

1. INTRODUCTION

The use of structured grids in reservoir simulation is very common in the petroleum industry. However, these grids present difficulties in representing complex geometries and locally refining near wells and faults. Although they cannot represent all details of geological reservoir models that should be incorporated into the numerical simulations, still little effort has been made in order to take advantage of numerical formulations that are able to deal with unstructured grids. These grids, composed by triangular and/or quadrilateral elements, for two-dimensional domains, are easier to conform, increasing the flexibility in representing reservoir geometries (Hurtado *et al.*, 2007a; Marcondes and Sepehrnoori, 2007).

One method that deals with unstructured grids is the so-called Control Volume Finite Element Method (CVFEM), developed at first for solving the Navier-Stokes equations. Unstructured elements can be used to represent complex geometries and to define the spatial variation of physical media properties, combining the flexibility of the Finite Element Method with local and global conservation enforcement, which is the essence of the Finite Volume Method. Hence, physical balances are made inside the control volumes, with contributions from different elements. Because of this principle, a better way to denominate the method would be Element-based Finite Volume Method (EbFVM), since it is a finite volume methodology that uses elements only as supporting entities, borrowing the concept of element and their shape functions from the finite element technique (Maliska, 2004).

In this work, an EbFVM applied to a chemical flooding compositional reservoir simulator is described. The formulation is applied for two-dimensional unstructured grids, considering triangular or quadrilateral elements or a combination of the two. Most of the ideas presented here were first employed by Raw (1985), when developing the FIELDS method for solving the Navier-Stokes equation. There are very few publications regarding the application of element-based finite volume methods for the numerical simulation of petroleum reservoirs. In the extent of multiphase flow in porous media is clear that we still need more efforts in order to take advantages of all features that unstructured grids can provide.

2. GENERAL DESCRIPTION OF THE SIMULATOR

The simulator considered in this work is called UTCHEM, developed at the University of Texas at Austin to simulate enhanced oil recovery methods using chemicals in combination, such as surfactant, polymer, and alkaline flooding (Delshad *et al.*, 1996).

The simulator is a multicomponent, multiphase, and compositional model to simulate chemical flooding processes and accounts for complex phase behavior and multiphase physical properties. Furthermore, it can model capillary pressures, three-phase relative permeabilities (water/gas/oil phases or water/oil/microemulsion phases), dispersion, diffusion, adsorption, chemical reactions, non-equilibrium mass transfer between phases and other related phenomena (UTCHEM-9.0, 2000). The solution method is implicit in pressure and explicit in concentration (IMPEC type). Originally, the formulation used to approximate the governing equations is the traditional finite volume method, often called finite difference method in the petroleum literature. As stated before, the implementation of a method that deals with unstructured grid, the EbFVM in this case, is the objective of this work, adding another key feature to the simulator.

3. MATHEMATICAL MODEL

In this section, a brief description of the model formulation is given. The description of phase behavior and physical property models is given elsewhere (Saad, 1989; Delshad *et al.*, 1996; UTCHEM-9.0, 2000). The fundamental equations are the mass balance equation for each species, the aqueous phase pressure, and the energy balance equation (not considered in this work). The aqueous phase pressure is obtained by an overall mass balance on volume-occupying components (water, oil, surfactant, co-solvent, and gas), while the other phase pressures are computed by adding the capillary pressure between phases.

3.1. Mass conservation equation

The continuity of mass for each component is expressed in terms of overall volume of component κ per unit pore volume ($\tilde{C}_\kappa$) as

$$\frac{\partial}{\partial t}\left(\phi \tilde{C}_\kappa \rho_\kappa\right) + \vec{\nabla}\cdot\left[\sum_{l=1}^{n_p} \rho_\kappa\left(C_{\kappa l}\vec{\mathbf{u}}_l - \vec{\mathbf{D}}_{\kappa l}\right)\right] = R_\kappa \tag{1}$$

The overall volume of component κ per unit of pore volume is the sum over all phases, including the adsorbed phases:

$$\tilde{C}_\kappa = \left(1 - \sum_{\kappa=1}^{n_{cv}} \hat{C}_\kappa\right)\sum_{l=1}^{n_p} s_l C_{\kappa l} + \hat{C}_\kappa \tag{2}$$

where n_{cv} is the total number of volume-occupying components, n_p is the number of phases, s_l is the phase saturation, $C_{\kappa l}$ is the concentration of component κ in phase l, $\hat{C}_\kappa$ is the adsorbed concentration of species κ, ρ_κ is the density of pure component κ, and $\vec{\mathbf{D}}_{\kappa l}$ is the dispersive flux, assumed to have a Fickian form (Bear, 1979).

The superficial velocity of each phase is related to the pressure gradient by Darcy's law for multiphase flow given by

$$\vec{\mathbf{u}}_l = -\frac{k_{rl}}{\mu_l}\vec{\vec{\mathbf{K}}}\cdot\left(\vec{\nabla}P_l - \gamma_l\vec{\nabla}h\right) \tag{3}$$

where P_l is the phase pressure, k_{rl} is the relative permeability, μ_l is the phase viscosity, $\vec{\vec{\mathbf{K}}}$ is the intrinsic permeability tensor, h is the vertical depth, and γ_l is the phase specific weight.

The source term R_κ in Eq. (1) is a combination of all rate terms for a particular component and may be expressed as

$$R_\kappa = \phi\sum_{l=1}^{n_p} s_l r_{\kappa l} + (1-\phi)r_{\kappa s} + Q_\kappa \tag{4}$$

where Q_κ is the injection or production rate for component κ per bulk volume and $r_{\kappa l}$ and $r_{\kappa s}$ are the reaction rates for component κ in phase l, and solid phase s, respectively.

3.1. Pressure equation

The pressure equation is developed by summing the mass balance equations over-all volume-occupying components, substituting Darcy's law for the phase velocity terms and using the definition of capillary pressure. Thus, the pressure equation for the aqueous phase results in the following equation:

$$\phi C_t \frac{\partial P_1}{\partial t} + \vec{\nabla} \cdot \left(\lambda_{rTc} \vec{\vec{K}} \cdot \vec{\nabla} P_1 \right) = -\vec{\nabla} \cdot \left(\sum_{l=1}^{n_p} \lambda_{rlc} \vec{\vec{K}} \cdot \gamma_l \vec{\nabla} h \right) + \vec{\nabla} \cdot \left(\sum_{l=1}^{n_p} \lambda_{rlc} \vec{\vec{K}} \cdot \vec{\nabla} P_{cl1} \right) + \sum_{\kappa=1}^{n_{cv}} Q_\kappa \tag{5}$$

with

$$\lambda_{rlc} = \frac{k_{rl}}{\mu_l} \sum_{\kappa=1}^{n_{cv}} \rho_\kappa C_{\kappa l} \tag{6}$$

and the total relative mobility including the correction for fluid compressibility given by

$$\lambda_{rTc} = \sum_{l=1}^{n_p} \lambda_{rlc} \tag{7}$$

The total compressibility C_t is the volume-weighted sum of the rock (C_r) and component compressibilities (C_κ^o):

$$C_t = C_r + \sum_{\kappa=1}^{n_{cv}} C_\kappa^o \tilde{C}_\kappa \tag{8}$$

4. NUMERICAL FORMULATION

The basic idea of any finite volume method is to divide the solution domain into smaller sub-domains, called control volumes, where the governing equations, Eqs. (1) and (5), are integrated and the conservation of physical quantities is guaranteed. In the EbFVM formulation, control volumes are assembled with contributions from different elements. The unknowns of the problem are calculated at points called nodes, or vertexes, located at every element corner. Therefore, in contrast to traditional finite volume methods, in the EbFVM elements and control volumes no longer coincide. In this formulation, control volumes are built around grid nodes, joining the center of the elements to its medians (cell vertex construction). The resulting control volume is formed by portions of the elements sharing a common node, as shown in Fig. 1.
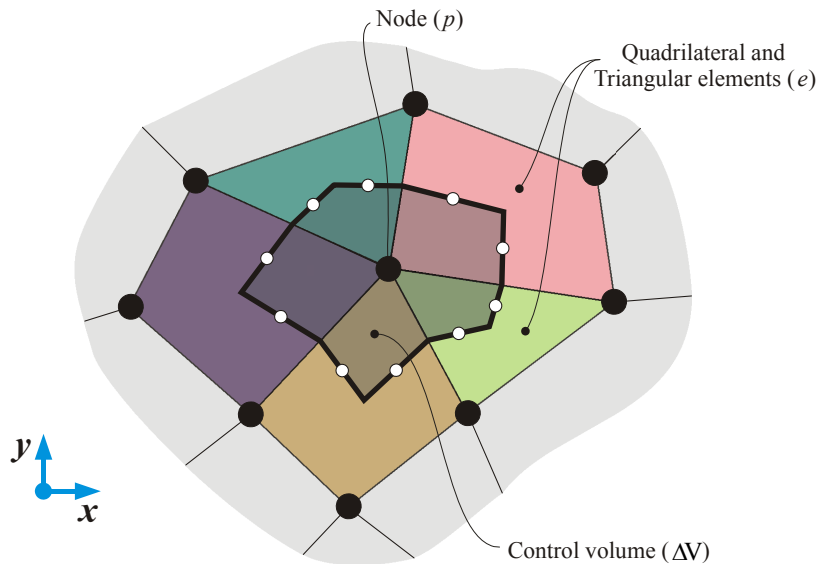

Figure 1. Control volume assembling in EbFVM

When joining the center of an element with the midpoint of the edges, sub-control volumes are created. The control volume is obtained with contributions from sub-control volumes sharing the same node. Every element sharing a common node contributes with one sub-control volume and with two faces to the control volume. The midpoint of each face is usually known as integration point, due to the midpoint rule approximation, with all fluxes being calculated at these points. Since in this formulation the elements are homogeneous, that is, properties such as porosity and permeability do not vary inside each element, there is no need to do any type of averaging procedure for calculating

these properties at integration points (Cordazzo, 2006). In this work, both triangular and quadrilaterals are considered, as depicted in Fig. 2.
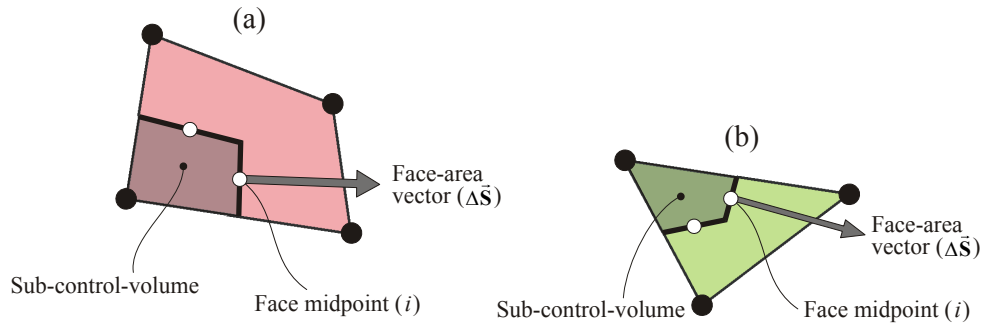

Figure 2. (a) Quadrilateral and (b) Triangular elements

In the EbFVM the equations can be solved in the computational domain using a standard element, triangular or quadrilateral, in a local coordinate system. This procedure is borrowed from the finite element method, where each element is treated identically and independently, no matter how complex the element geometry is in the global coordinates. By doing so, the conservation equations for each control volume can be simply assembled with contributions from the neighboring elements. Figure 3 shows the coordinate transformation for triangles and quadrilaterals.
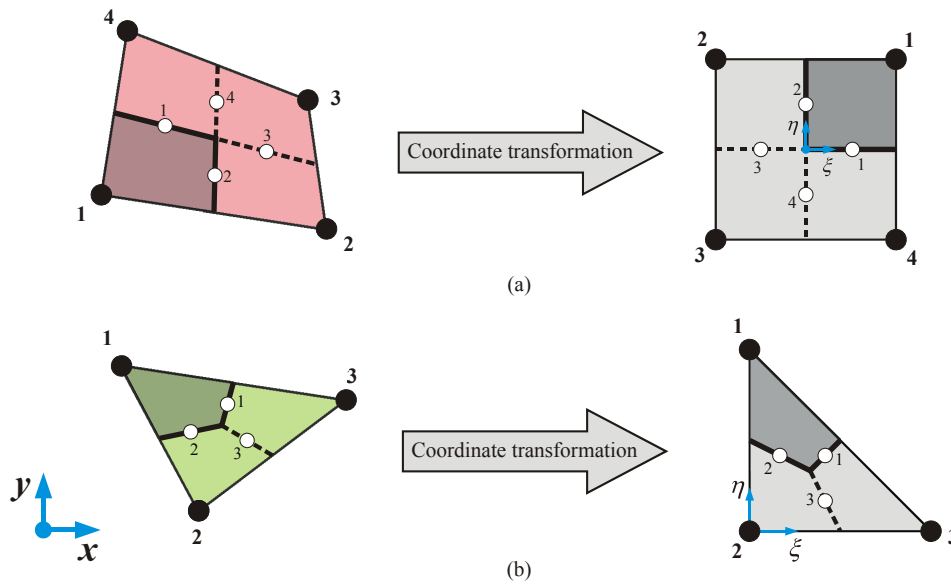

Figure 3. (a) Quadrilateral and (b) Triangular elements represented in global and local coordinate systems

Any physical property inside an element can be expressed in terms of its linear (triangle) or bilinear (quadrilateral) shape functions and the property values in the element nodes. That is,

$$\Theta(\xi,\eta) = \sum_{j=1}^{nne} N_j(\xi,\eta)\Theta_j \tag{9}$$

where nne is the number of nodes per element (3 for triangles and 4 for quadrilaterals), Θ_j are the nodal values for the property and N_j are the element shape functions, defined for triangles as

$$\begin{cases} N_1(\xi,\eta) = 1 - \xi - \eta \\ N_2(\xi,\eta) = \xi \\ N_3(\xi,\eta) = \eta \end{cases} \tag{10}$$

and for quadrilateral as

$$
\begin{cases}
N_1(\xi,\eta) = \dfrac{1}{4}(1+\xi)(1+\eta) \\[2mm]
N_2(\xi,\eta) = \dfrac{1}{4}(1-\xi)(1+\eta) \\[2mm]
N_3(\xi,\eta) = \dfrac{1}{4}(1+\xi)(1-\eta) \\[2mm]
N_4(\xi,\eta) = \dfrac{1}{4}(1-\xi)(1-\eta)
\end{cases}
\tag{11}
$$

In order to evaluate fluxes at faces inside an element, usually it is necessary to approximate the gradient of the variable of interest at integration points. The following approximation is used to evaluate the gradient of a generic variable Θ inside the element:

$$
[\nabla\Theta]_i = [J]_i^{-1}[D]_i[\Theta]_e
\tag{12}
$$

where $[\Theta]_e$ is the vector containing the values of the given variable at the element nodes, $[D]_i$ is the first-order partial derivatives of the shape functions written in a matrix form as

$$
[D]_i = \begin{bmatrix} \partial_\xi N_1 & \cdots & \partial_\xi N_{nne} \\ \partial_\eta N_1 & \cdots & \partial_\eta N_{nne} \end{bmatrix}
\tag{13}
$$

In Eq. (12), the Jacobian matrix of the coordinate transformation, $[J]_i$, can be easily calculated by

$$
[J]_i = [D]_i[\Omega]_e
\tag{14}
$$

where $[\Omega]_e$ is a matrix containing the global coordinates of the nodes inside element e, as the form

$$
[\Omega]_e = \begin{bmatrix} x_1 & y_1 \\ \vdots & \vdots \\ x_{nne} & y_{nne} \end{bmatrix}
\tag{15}
$$

Similar relationships can be obtained for any geometric parameter needed for the discretization process (Hurtado, 2005).

4.1. Integration of the pressure equation

As stated before, we must integrate Eqs. (1) and (5) in order to apply the mass conservation for each control volume. First, disregarding the gravitational effect, the integration of the pressure equation leads to

$$
\int_{V,t} \phi C_t \frac{\partial P_1}{\partial t} dVdt + \int_{V,t} \vec{\nabla}\cdot\left(\lambda_{rTc}\vec{\vec{\mathbf{K}}}\cdot\vec{\nabla}P_1\right)dVdt = \int_{V,t} \vec{\nabla}\cdot\left(\sum_{l=1}^{n_p}\lambda_{rlc}\vec{\vec{\mathbf{K}}}\cdot\vec{\nabla}P_{cl1}\right)dVdt + \int_{V,t}\sum_{\kappa=1}^{n_{cv}}Q_\kappa dVdt
\tag{16}
$$

Applying the divergence theorem to Eq. (16) for both the second term of the LHS and the first term of the RHS, we have

$$
\int_{V,t} \phi C_t \frac{\partial P_1}{\partial t} dVdt + \int_{S,t}\left(\lambda_{rTc}\vec{\vec{\mathbf{K}}}\cdot\vec{\nabla}P_1\right)\cdot\mathbf{d\vec{S}}dt = \int_{S,t}\left(\sum_{l=1}^{n_p}\lambda_{rlc}\vec{\vec{\mathbf{K}}}\cdot\vec{\nabla}P_{cl1}\right)\cdot\mathbf{d\vec{S}}dt + \int_{V,t}\sum_{\kappa=1}^{n_{cv}}Q_\kappa dVdt
\tag{17}
$$

where the surface integrals are performed over-all faces of the control volume. Approximating these integrals by means of the midpoint rule is possible to derive a discrete expression at time level n:

$$\phi_p \Delta V_p \left(C_t\right)_p^n \frac{\left[\left(P_1\right)_p^n - \left(P_1\right)_p^{n-1}\right]}{\Delta t} + \sum_e \left\{\sum_i \left(\lambda_{rTc}\right)_i^n \left[\vec{\mathbf{K}} \cdot \left(\vec{\nabla} P_1\right)_i^n\right] \cdot \Delta \vec{\mathbf{S}}_i\right\}_e =$$
$$\sum_e \left\{\sum_i \sum_{l=1}^{n_p} \left(\lambda_{rlc}\right)_i^n \left[\vec{\mathbf{K}} \cdot \left(\vec{\nabla} P_{cl1}\right)_i^n\right] \cdot \Delta \vec{\mathbf{S}}_i\right\}_e + \sum_{\kappa=1}^{n_{cv}} \left(\Delta V Q_\kappa\right)_p \tag{18}$$

Here, the surface integrals are approximated by the means of the midpoint rule and the time derivative is approximated by an expression of finite difference. Equation (18) refers to the control volume around node p, with volume equal to ΔV_p, and is formed by contributions from different elements e (outer summation). On the other hand, in two-dimensional domains each element contributes with two integration points i over a control surface (inner summation). Moreover, $\Delta \vec{\mathbf{S}}_i$ denotes the face area vector, pointing outside of the control volume, as shown in Fig. 2.

The gradient terms in Eq. (18) can be computed applying the approximation given by Eq. (12). Thus, one can show that is possible to write the following term

$$\sum_e \left\{\sum_i \left(\lambda_{rTc}\right)_i^n \left[\vec{\mathbf{K}} \cdot \left(\vec{\nabla} P_1\right)_i^n\right] \cdot \Delta \vec{\mathbf{S}}_i\right\}_e = \sum_e \sum_i \left(\lambda_{rTc}\right)_i^n [b]_i^T [P_1]_e^n \tag{19}$$

for the pressure gradient, and

$$\sum_e \left\{\sum_i \sum_{l=1}^{n_p} \left(\lambda_{rlc}\right)_i^n \left[\vec{\mathbf{K}} \cdot \left(\vec{\nabla} P_{cl1}\right)_i^n\right] \cdot \Delta \vec{\mathbf{S}}_i\right\}_e = \sum_e \sum_i \sum_{l=1}^{n_p} \left(\lambda_{rlc}\right)_i^n [b]_i^T [P_{cl1}]_e^n \tag{20}$$

for the capillary pressure gradient term for the integration point i inside element e. In the previous equations, $[P_1]_e^n$ and $[P_{cl1}]_e^n$ are the vector of pressure nodal values and the vector of capillary pressure in the element e (dimension of nne), respectively. The term $[b]_i^T$ is a vector defined as

$$[b]_i^T = [\Delta S]_i^T [K]_e [J]_i^{-1} [D]_i \tag{21}$$

where $[\Delta S]_i$ is the face area vector, $[K]_e$ is the permeability tensor for the element expressed in a matrix form, while $[J]_i$ and $[D]_i$ are defined in Eqs. (14) and (13), respectively.

Substituting Eqs. (19) and (20) into Eq. (18) we obtain the complete form of the discrete pressure equation:

$$\phi_p \Delta V_p \left(C_t\right)_p^n \frac{\left[\left(P_1\right)_p^n - \left(P_1\right)_p^{n-1}\right]}{\Delta t} + \sum_e \sum_i \left(\lambda_{rTc}\right)_i^n [b]_i^T [P_1]_e^n = \sum_e \sum_i \sum_{l=1}^{n_p} \left(\lambda_{rlc}\right)_i^n [b]_i^T [P_{cl1}]_e^n + \sum_{\kappa=1}^{n_{cv}} \left(\Delta V Q_\kappa\right)_p \tag{22}$$

4.2. Integration of the concentration equation

Since an IMPEC formulation is used in the simulator, for every time step the aqueous phase pressure is solved implicitly and the component overall concentrations are solved explicitly, right after solving the pressure equation. Thus, we can evaluate the overall concentration for each species at time level $n+1$ integrating Eq. (1), as follows:

$$\int_{V,t} \frac{\partial}{\partial t} \left(\phi \tilde{C}_\kappa \rho_\kappa\right) dV dt + \int_{V,t} \vec{\nabla} \cdot \left[\sum_{l=1}^{n_p} \rho_\kappa \left(C_{\kappa l} \vec{\mathbf{u}}_l - \vec{\tilde{\mathbf{D}}}_{\kappa l}\right)\right] dV dt = \int_{V,t} R_\kappa dV dt \tag{23}$$

Evaluating the terms in a similar way as in the pressure equation, we obtain

$$\left(\tilde{C}_\kappa\right)_p^{n+1} = \left(\tilde{C}_\kappa\right)_p^n - \frac{\sum_e \sum_i \sum_{l=1}^{n_p} \left[\left(C_{\kappa l}\right)_i^n \left(q_l\right)_i^n - \left(D_{\kappa l}\right)_i^n\right]}{\phi_p \Delta V_p} \Delta t + \left(\frac{R_\kappa}{\phi \rho_\kappa}\right)_p \Delta t . \tag{24}$$

where the flux across a face is given by

$$\left(q_l\right)_i^n = -\left(\lambda_{rlc}\right)_i^n [b]_i^T [P_1]_e^n \tag{25}$$

4.3. Spatial interpolation scheme

The technique commonly used for spatial interpolation of mobility terms in Eqs. (22) and (25) is the upwind-type interpolation scheme. In this work, for triangular and quadrilateral elements, a single-point upwind scheme is used, where the upstream weighting of the mobility in each face is determined analyzing whether the flux across the face is positive or not (Cordazzo, 2006). However, this scheme can provide significant grid orientation effect, as it does not consider the actual flow direction into the numerical approximations of the advective terms. In order to avoid this undesirable effect, other schemes that take into account the true direction of the flow could be used (Hurtado *et al.*, 2007b).

5. NUMERICAL RESULTS

In this section, two examples are analyzed. The first one is the well known five-spot well pattern, divided into two test cases: a water flooding and a surfactant/polymer flooding case. The solution obtained in both cases employing the new implementation (EbFVM) is compared to the solution obtained with the original simulator, which employs the traditional finite difference method (FDM). On the other hand, the second example is a synthetic case, where is shown the ability of the formulation in dealing with more complex reservoir geometries discretized with fully unstructured grids and local grid refinements. In UTCHEM, this mesh cannot be represented using the original method. However, this geometry can be easily handled with the element-based formulation implemented in this work.

For the sake of simplicity, we assumed incompressible rock and fluids, no chemical reactions, no adsorptions, zero capillary pressure. These effects do not depend on the method used to discretize the equations, as they do not require any geometric information, and were neglected for the purpose of model validation.

5.1. Validation

The objective of this example is to show that the EbFVM is correctly implemented into the chemical simulator, providing results that are in agreement with original solutions.

Different meshes were used for the EbFVM and for the FDM, as shown in Fig. 4. For the original method (Fig. 4a), a structured grid with 24x24 control volumes (gridblocks) is used, while for the new method (Fig. 4b) a mesh with 60 triangular elements and 414 quadrilateral elements is used, resulting in 485 control volumes.
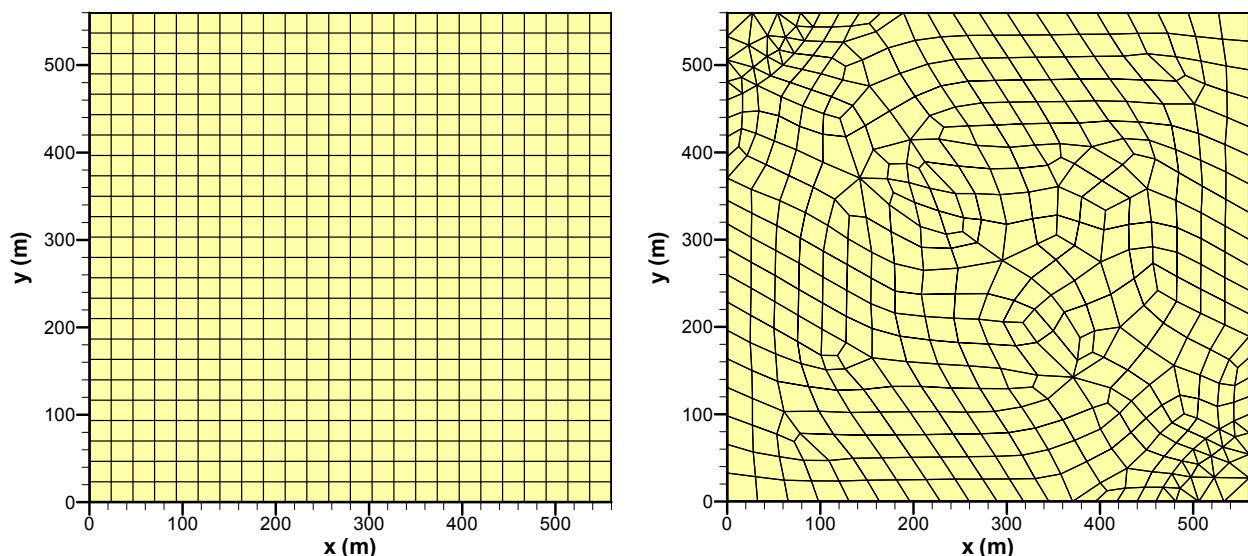

Figure 4. (a) Structured grid used with FDM and (b) Unstructured hybrid grid used with EbFVM

The meshes shown in Fig. 4 were used to simulate two case studies. The first one is a water flooding case and the second case is a chemical flood, where surfactant and polymer are added to the injected water. The wells are located in the left-upper corner and in the right-down corner as a quarter of five spot well pattern. Figure 5a compares the cumulative oil recovery for both methods and both cases, while Fig. 5b shows the oil phase cut. The original solution is plotted in solid lines and the solution of EbFVM is plotted with symbols.
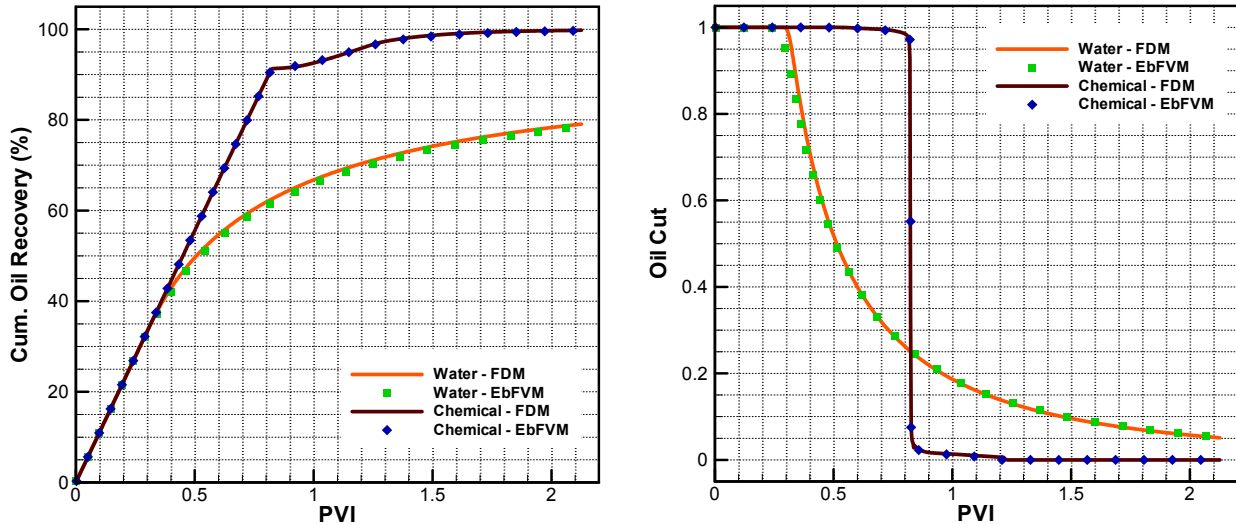
Figure 5. (a) Cumulative oil recovery and (b) Oil cut for both methods and cases in the production well

Comparing the water and chemical flooding results, it is clear that when surfactant and polymer are injected, the oil recovery is remarkably enhanced, with a much sharper fluid front. Enhanced oil recovery processes such the one considered above have utilized polymer to reduce fluid mobility to improve the sweep efficiency of the reservoir, i.e., to increase the volume of the permeable medium contacted at any given time (Lake, 1989; Sorbie, 1991).

On the other hand, comparing the solutions between the two methods, we can see that the results obtained with EbFVM are in excellent agreement with the results from the FDM, even using a coarse and unstructured grid for a case that has symmetric solution.

5.2. Mesh refinement example

In this case, a more realistic enhanced oil recovery simulation is carried out. Reservoirs with more complex geometry can be modeled with great flexibility with the proposed numerical technique. The triangular unstructured grid used for discretizing this reservoir is shown in Fig. 6. Local grid refinement around the wells is considered for a more accurate solution in those locations. As stated before, this is one of the main advantages of the element-based method, i.e., avoids mesh refinement in unnecessary regions as occurs with the traditional finite-volume method.
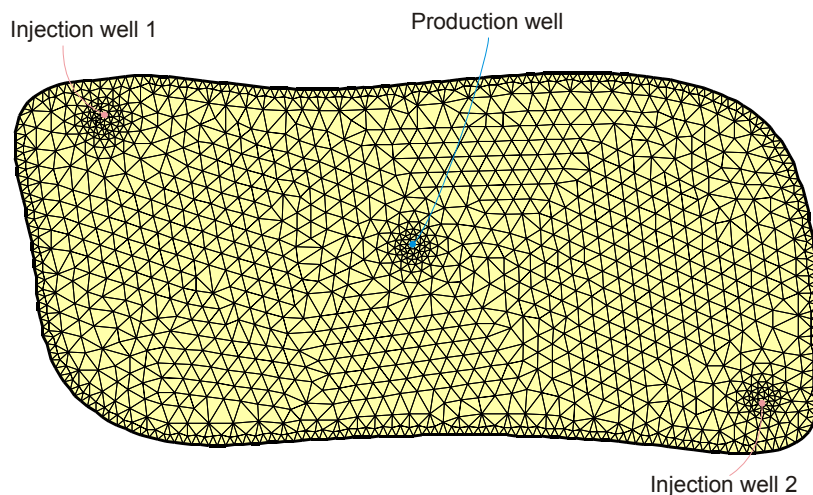

Figure 6. Unstructured grid with local refinement

For this case, surfactant, polymer, and water are injected in the injection well 1 and only water is injected at well 2. The injection rate is $2.8 \, \mathrm{m^3/d}$ per well and the bottom-hole pressure of production well is $690 \, \mathrm{kPa}$. In the first well the concentration of surfactant is 3 vol% (97% water) and the concentration of polymer is equal to 2000 ppm (0.2 wt%). Reservoir properties are assumed to be homogeneous and isotropic, with absolute permeability of 100 mD and porosity of 0.2.

Figure 7 shows the water concentration map at four different injection times. One can note that the simulation provides results that are qualitatively reproducing the expected physical behavior, with nearly radial front in the injection wells.
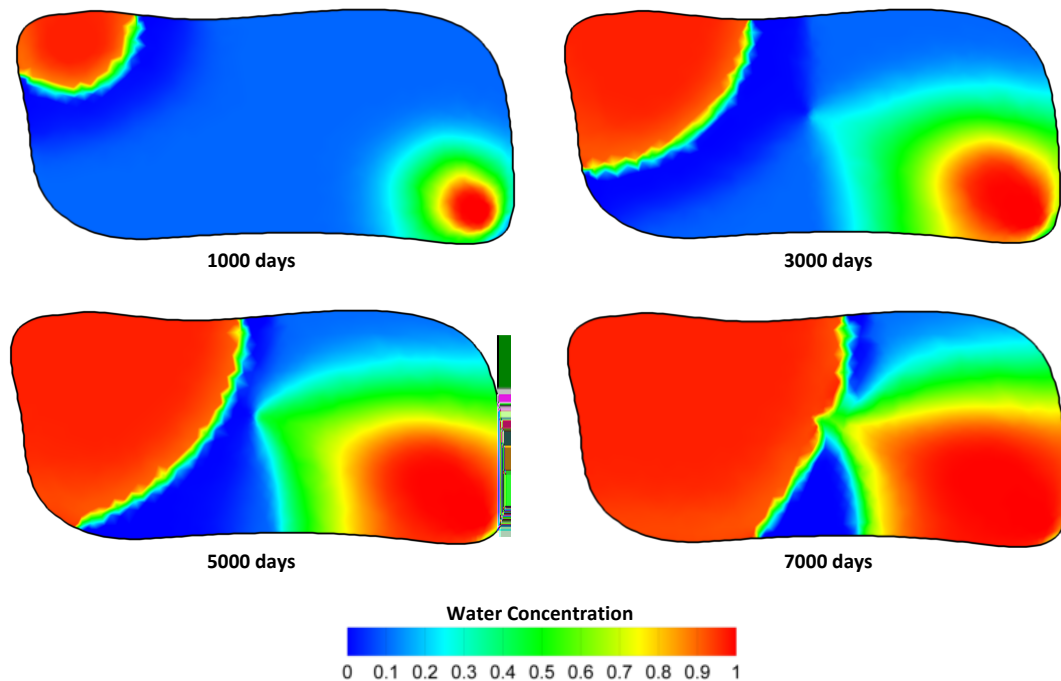

1000 days

3000 days

5000 days

7000 days

Water Concentration

0   0.1 0.2 0.3 0.4 0.5 0.6 0.7 0.8 0.9 1

Figure 7. Water concentration profile in different simulation times

6. CONCLUSIONS

An element-based finite volume formulation using triangular and/or quadrilateral unstructured grids in conjunction with a chemical flooding compositional reservoir simulator was presented in this paper. Although only two-dimensional domains were considered in this work, the extension to three-dimensional domains is straightforward, since the substantial changes are related to the shape functions, according to the element type considered, and they are available in several publications regarding finite element method.

The formulation presented has two major advantages over traditional methodologies used in the petroleum industry. First, it has increased geometrical flexibility for representing complex reservoir geometries, with the possibility of local grid refinement in regions of interest. This can be done naturally, with a smooth transition between refined and coarse regions, without the difficulties found in structured meshes. The second is that this method can deal with the heterogeneous and full tensor permeability without any additional complexity in the formulation such as averaging procedures along the control volume faces, since this scheme assumes uniform properties inside elements.

Although the validation was presented for only two test cases, water and chemical flooding, and only one mesh was used for each method, the EbFVM implementation on UTCHEM has been tested for numerous cases with more complex reservoir and fluid properties. All these tests indicated that the method was successfully implemented and that it can perfectly substitute the traditional finite difference method, since the results are always in good agreement for both solutions. Furthermore, so far no restrictions were found regarding the EbFVM applicability. A second example was carried out, in order to show the flexibility of the element-based formulation, describing a more complex reservoir geometry and applying local grid refinement around wells.

7. REFERENCES

Bear, J., 1979, "Hydraulics of Ground Water", McGraw Hill, New York, USA.

Cordazzo, J., 2006, "Petroleum Reservoir Simulation Using EbFVM and Algebraic Multigrid", Doctoral Dissertation (in Portuguese), Mechanical Engineering Department, Federal University of Santa Catarina, Florianópolis, Brazil.

Delshad, M., Pope, G. A. and Sepehrnoori, K., 1996, "A Compositional Simulator for Modeling Surfactant Enhanced Aquifer Remediation", Journal of Contaminant Hydrology, 23, 303-327.

Hurtado, F. S. V., 2005, "An Element-based Finite Volume Formulation for Numerical Simulation of Two-Phase Immiscible Displacement in Porous Media", M.Sc. Thesis (in Portuguese), Federal University of Santa Catarina, Florianópolis, Brazil.

Hurtado, F. S. V., Maliska, C. R., Silva, A. F. C. and Cordazzo, J., 2007, "A Quadrilateral Element-based Finite Volume Formulation for the Simulation of Complex Reservoirs", Paper SPE 107444, X Latin American and Caribbean Petroleum Engineering Conference, Buenos Aires, Argentina.

Hurtado, F. S. V., Maliska, C. R. and Silva, A. F. C., 2007, "On the Factors Influencing the Grid Orientation Effect in Reservoir Simulation", Proceedings of COBEM 2007, Brasília, Brazil.

Lake, L. W., 1989, "Enhanced Oil Recovery", Prentice-Hall, Inc., Englewood Cliff, USA.

Maliska, C. R., 2004, "Computational Heat Transfer and Fluid Flow", 2nd Edition (in Portuguese), Livros Técnicos e Científicos Editora S.A., Rio de Janeiro, Brazil.

Marcondes, F. and Sepehrnoori, K., 2007, "Unstructured Grids and an Element Based Conservative Approach for Compositional Reservoir Simulation", Proceedings of COBEM 2007, Brasília, Brazil.

Raw, M., 1985, "A New Control Volume Based Finite Element Procedure for the Numerical Solution of the Fluid Flow and Scalar Transport Equations", Ph.D. Dissertation, University of Waterloo, Waterloo, Canada.

Saad, N., 1989, "Field Scale Studies With a 3-D Chemical Flooding Simulator", Ph.D. Dissertation, The University of Texas at Austin, Austin, USA.

Sorbie, K. S., 1991, "Polymer-Improved Oil Recovery", CRC Press, Inc., Boca Raton, USA.

UTCHEM-9.0, 2000, "Technical Documentation for UTCHEM-9.0: a Three-Dimensional Chemical Flood Simulator", Reservoir Engineering Research Program, Center for Petroleum and Geosystems Engineering, The University of Texas at Austin, Austin, USA.

8. RESPONSIBILITY NOTICE

The authors are the only responsible for the printed material included in this paper.